

Provided for non-commercial research and education use.  
Not for reproduction, distribution or commercial use.



(This is a sample cover image for this issue. The actual cover is not yet available at this time.)

**This article appeared in a journal published by Elsevier. The attached copy is furnished to the author for internal non-commercial research and education use, including for instruction at the authors institution and sharing with colleagues.**

**Other uses, including reproduction and distribution, or selling or licensing copies, or posting to personal, institutional or third party websites are prohibited.**

**In most cases authors are permitted to post their version of the article (e.g. in Word or Tex form) to their personal website or institutional repository. Authors requiring further information regarding Elsevier's archiving and manuscript policies are encouraged to visit:**

**<http://www.elsevier.com/copyright>**



Contents lists available at SciVerse ScienceDirect

## Science of the Total Environment

journal homepage: [www.elsevier.com/locate/scitotenv](http://www.elsevier.com/locate/scitotenv)

## Tracking the complete revolution of surface westerlies over Northern Hemisphere using radionuclides emitted from Fukushima

M.A. Hernández-Ceballos<sup>a</sup>, G.H. Hong<sup>b</sup>, R.L. Lozano<sup>a</sup>, Y.I. Kim<sup>c</sup>, H.M. Lee<sup>b</sup>, S.H. Kim<sup>b</sup>, S.-W. Yeh<sup>d</sup>, J.P. Bolívar<sup>a,\*</sup>, M. Baskaran<sup>e</sup>

<sup>a</sup> Department of Applied Physics, University of Huelva, Huelva, Spain

<sup>b</sup> Korea Ocean Research and Development Institute, Ansan 426–744, South Korea

<sup>c</sup> Korea Ocean Research and Development Institute, Ulsjin 767–813, South Korea

<sup>d</sup> Department of Environmental Marine Science, Hanyang University, Ansan, 426–791, South Korea

<sup>e</sup> Department of Geology, Wayne State University, Detroit, Michigan, USA

### HIGHLIGHTS

- ▶ Evidence of the South Korea contamination with released radiocesium from Fukushima.
- ▶ Field samples and air mass analysis were utilized to elucidate the transport of those radionuclides.
- ▶ Characterization of the air mass movements at different sites at the Earth's surface.
- ▶ Verification of the uninterrupted complete revolution of the artificial radionuclides released in Fukushima.
- ▶ Quantification of the velocity of the artificial radionuclides released in Fukushima.

### ARTICLE INFO

#### Article history:

Received 17 April 2012

Received in revised form 13 July 2012

Accepted 6 August 2012

Available online xxxx

#### Keywords:

Fukushima

<sup>134</sup>Cs

Atmosphere

Air masses

Westerlies

Northern Hemisphere

### ABSTRACT

Massive amounts of anthropogenic radionuclides were released from the nuclear reactors located in Fukushima (northeastern Japan) between 12 and 16 March 2011 following the earthquake and tsunami. Ground level air radioactivity was monitored around the globe immediately after the Fukushima accident. This global effort provided a unique opportunity to trace the surface air mass movement at different sites in the Northern Hemisphere. Based on surface air radioactivity measurements around the globe and the air mass backward trajectory analysis of the Fukushima radioactive plume at various places in the Northern Hemisphere by employing the Hybrid Single-Particle Lagrangian Integrated Trajectory model, we show for the first time, that the uninterrupted complete revolution of the mid-latitude Surface Westerlies took place in less than 21 days, with an average zonal velocity of >60 km/h. The position and circulation time scale of Surface Westerlies are of wide interest to a large number of global researchers including meteorologists, atmospheric researchers and global climate modellers.

© 2012 Elsevier B.V. All rights reserved.

### 1. Introduction

Surface westerlies are a dominant feature in the mid-latitudes of the Northern Hemisphere throughout the year. The speed of the westerlies increases from the land or sea surface to higher altitudes because of a strong temperature gradient in the meridional direction in the mid-latitudes. Meteorological measurements and analysis of climate data can be used to calculate wind fields and back trajectories of air parcels by running atmospheric models in reverse to determine the wind fields resulting from synoptic conditions, and hence the

general source of, and path taken by, an air mass that crossed a given region of interest. Various tracers of natural and man-made materials (e.g., sulphur isotopes, metals, radionuclides) have been used to verify the meteorological models in recent decades. Trade wind circulation in the lower latitude was successfully traced earlier based on the dispersal of radionuclides emitted from the nuclear weapon tests at or near the earth's surface near the equator in 1952 and 1954 (Machta et al., 1956). The high altitude westerlies in the mid-latitudes over the Northern Hemisphere were also successfully traced by the presence of Asian dust originated from the central Asia (~40°N, 88°E) embedded in the glaciers of Greenland and French Alps as well as the bottom of the North Pacific Ocean (Steffensen et al., 2008; Uno et al., 2009). However, surface westerlies travel mostly in the lower troposphere and are often disrupted due to the uneven distribution of synoptic scale atmospheric pressure systems; therefore more than

\* Corresponding author at: University of Huelva, Campus de El Carmen, 21071, Huelva, Spain. Tel.: +34 959219793; fax: +34 959219777.

E-mail address: [bolivar@uhu.es](mailto:bolivar@uhu.es) (J.P. Bolívar).

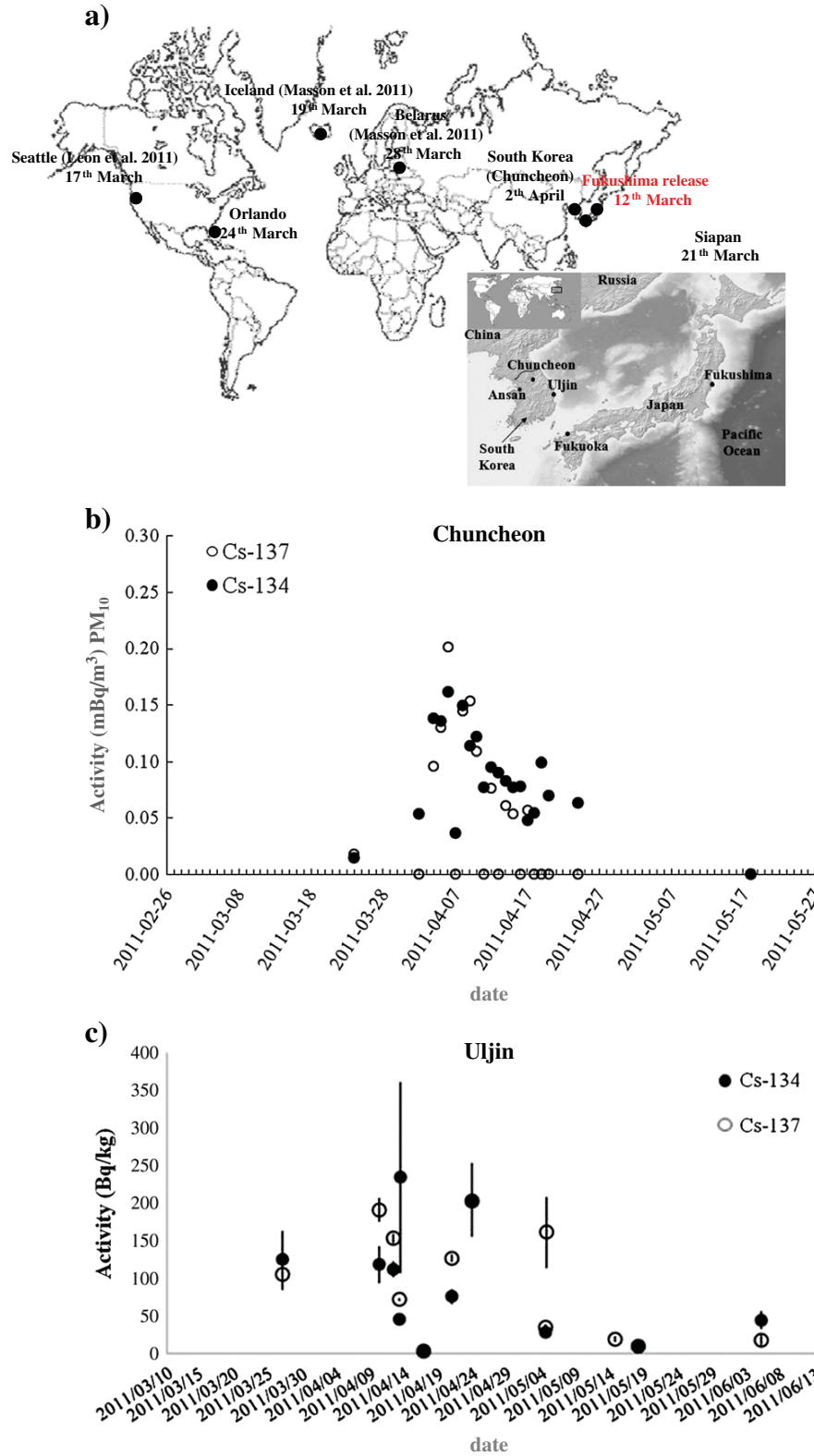


**Fig. 1.** (a) First arrival date of Fukushima radioactive substances at various sites in the northern Hemisphere. (b) Atmospheric aerosol concentration of <sup>134</sup>Cs and <sup>137</sup>Cs in Chuncheon, South Korea (data from Korea Institute of Nuclear Safety website). The aerosol was collected at 09:00 am every morning for the next 24 hours on to a glass fiber filter using a high volume sampler (Kim et al., 2011). (c) <sup>134</sup>Cs and <sup>137</sup>Cs activity concentration in dust falling on the ground during March to June 2011 in Uljin, Korea. Error bars arise from 1- sigma counting statistics.

one full revolution has rarely been verified so far with material tracers.

A rare opportunity to trace the pathways of the surface westerlies was presented by the sudden release of artificial radionuclides from the damaged Fukushima nuclear reactors stricken by a great earthquake and tsunami-driven flooding on 11 March 2011. The Fukushima Daiichi complex was affected by a tsunami that hit the east coast of Japan, caused by a 9.0 magnitude earthquake in the Pacific Ocean (epicentre 38.32°N, 142.37°E) which was the largest earthquake in modern times in the northeast of Japan (Minoura et al., 2001). The emission of certain fission products (e.g.,  $^{35}\text{S}$ ,  $^{131}\text{I}$ ,  $^{134}\text{Cs}$ , and  $^{137}\text{Cs}$ ) to the atmosphere occurred immediately after the flooding of the reactors, peaked on March 15–16 and virtually stopped after March 17 with occasional smaller subsequent emission (Lozano et al., 2011; Priyadarshi et al., 2011). Aerosol sampling networks in the Northern Hemisphere registered that the Fukushima radioactive plume of  $^{134}\text{Cs}$  and  $^{137}\text{Cs}$  arrived in California on March 18 (US EPA, 2011), and in Western Europe on March 19 (Masson et al., 2011). In South Korea, the arrival of radionuclides was well detected from 1–3 April (Fig. 1b–c). Dust fell on the ground at Uljin was contaminated with Fukushima-derived radio-cesium with elevated levels of  $^{137}\text{Cs}$  >200 Bq/kg (Fig. 1c). The concentrations of  $^{137}\text{Cs}$  in surface soil in South Korea prior to Fukushima accident was reported to be about 50 Bq/kg (dry wt.) (Lee et al., 1995). Therefore, the air mass surrounding South Korea and Kyushu Island appeared to be disconnected from the northeast coast of Japan, i.e., Fukushima Daiichi nuclear power plants, for the period of 11 March until the end of that month (Momoshima et al., 2012).

However, in late March, lower measurements of  $^{134}\text{Cs}$  and  $^{137}\text{Cs}$  were registered in Chuncheon (KINS, 2011) (Fig. 1b) and in Uljin (Fig. 1c). The simulation performed by the specific version of the numerical atmospheric chemistry and transport model Polyphemus/Polair3D (<http://cerea.enpc.fr/en/fukushima.html>) displays that these lower concentrations were derived by the progressive downward movement of radionuclides released from Fukushima and then accumulated in upper latitudes (Hong et al., in press).

A global network of ground air radioactivity monitoring in the Northern Hemisphere registered that contamination from the Fukushima accident dispersed from Asia to Europe (Fukushima→USA→Europe) and to South Korea with very similar atmospheric air  $^{134}\text{Cs}$  activity concentration (~0.3 mBq m<sup>-3</sup>) outside of Japan by the end of March (Lozano et al., 2011; KINS, 2011). However, the arrival of the radioactive plume over East Asia has not been reported in literature.

In this paper, a complete global revolution of surface westerlies was tracked using Fukushima emitted radionuclides taking advantage of global coverage of atmospheric radionuclides monitoring after Fukushima Daiichi Nuclear Power Plant accidents. South Korean observation was strategically chosen as it is located in the immediately westward from the Fukushima-Daiichi, therefore, the complete revolution of surface westerlies could be verified by tracking Fukushima radioactivity plume. Our results appear to be the first evidence of a complete uninterrupted global revolution of a radioactive plume due to Surface Westerlies at mid-latitudes in the Northern Hemisphere.

## 2. Materials and Methods

Wet and dry fallout were routinely collected at the eastern coast, Uljin (37° 04'32.02"N, 129°24' 19"E, East coast facing Japan) of the Korean Peninsula (Fig. 1). Uljin is located at about the same latitude as Fukushima (37° 18' 56" N, 141° 1' 33" E). The surface area of the deployed rain and dust collectors ranged between 0.5 and 5 m<sup>2</sup>. Dust samples were directly counted in a HPGe gamma spectrometer (Hong et al., 2006) and the cpm was converted to dpm using standard sources of  $^{134}\text{Cs}$  and  $^{137}\text{Cs}$  from Eckert & Ziegler and Isotope Products Laboratories which are traceable to the standard reference materials obtained from the National Institute of Standard and Technology.

The air mass analysis at the reference sites was based on the calculation of three-dimensional (3D) backward trajectories using the Hybrid Single-Particle Lagrangian Integrated Trajectory (HYSPLIT, version 4.9) model (Draxler et al., 2009) for an elevation of 1000 m above the model topography and 192 hours (8 days) prior to the arrival time. Model-calculated vertical velocities were used to compute backward trajectories, and the Global Data Assimilation System (GDAS) meteorological data set (reprocessed from NOAA's National Centres for Environmental Prediction Final Analysis data by Air Resources Laboratory) (information available online at <http://ready.arl.noaa.gov/archives.php>; Gridded Meteorological Data Archives) and the European Centre for Medium-Range Weather Forecasts (ECMWF) meteorological information were applied as meteorological input for the trajectory model. The GDAS files have a spatial resolution of 1° x 1° in latitude (111 km x 111 km), enough to resolve the air mass movement and its impact on global and synoptic transport, while the ECMWF with a spatial resolution of 0.25° in latitude (28 km x 28 km) were used to resolve the mesoscale and local transport in the sampling area (Seinfeld and Pandis, 2006). Hourly 3D backward trajectories were computed from 11th March to 30th April 2011 in order to avoid the large uncertainty and limited significance of a single backward trajectory (Stohl, 1998), and to achieve a more reliable representation of the synoptic airflow in the given region (Fig. 1a).

After the computation of the back trajectories, cluster techniques are used to extract patterns that help simplify and understand a large quantity of information, in order to minimize the subjectivity of the classifications obtained. This methodology is based on grouping similar objects together whereby differences among individual elements in a cluster are minimized and differences among clusters are maximized. HYSPLIT model uses a cluster analysis tool based on variations of the total spatial variance (TSV) between the different clusters formed and the spatial variance (SPVAR) between each cluster component (Draxler et al., 2009). The optimal number of clusters is defined as the number of clusters that best represent the air mass variability during one time period. This number is associated with the "break point", in which the TSV value increases rapidly, indicating that the clusters being combined are not very similar (Stunder, 1996). This increase suggests where to stop the clustering and, so, the optimal number of cluster is the step before the large increase in TSV. In this case, the "break point" has been associated with the first variation of the TSV above 40% (Hernández-Ceballos et al. in revision). Applying these criteria the optimal number of clusters is 5 (Fig. 2c) which show the prevalence of westerly flows over South Korea from 11th March to 5th April 2011.

## 3. Results and Discussion

A complete set of hourly backward trajectories at a final height of 1000 m at Uljin from 11th March to 5th April, each covering a previous time period of 192 hours (8 days), was reproduced from the beginning of the Fukushima nuclear power plant accident (Fig. 2a) in order to characterize the synoptic air mass behaviour over the sampling area. This height of 1000 m was chosen as a reference altitude after analysing the air mass behaviour at several levels including 500 m and 1500 m and checking that there were no significant variations in the air mass behaviour at each of these levels. During the early period after the accident (11th March–5th April), the backward trajectory analysis, represented as trajectory clusters, indicated a dominance of westerly flows over South Korea, indicating the homogeneous air masses without large zonal variations from Europe to Asia, and Fukushima derived radio-cesium via the surface westerlies was estimated to have arrived in 1–3 April for the first time in South Korea (Fig. 2c). The hourly analysis of 72 h backward trajectories at the height of 200 m (Fig. 2b) during the same period also indicated that the air over South Korea was not under the influence of the air over the areas adjacent to the Fukushima Daiichi nuclear plant (Fig. 2b). South Korea had received very little Fukushima radioactive plume during this period. Our

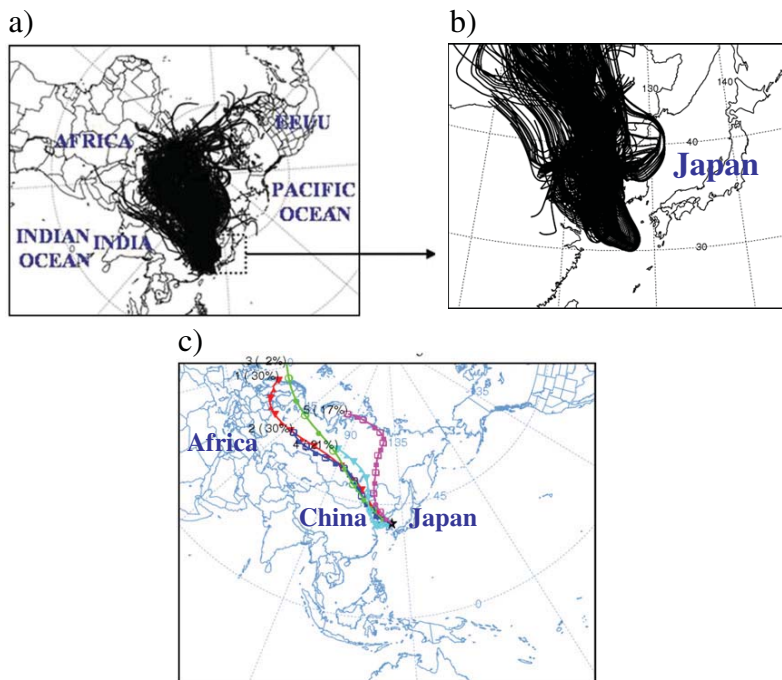


**Fig. 2.** a) Hourly backward trajectories at 1000 m (computed with GDAS files) and b) at 200 m (computed with ECMWF files) and c) the corresponding clusters at 1000 m during 11th March-5th April over Uljin (South Korea). In the clusters figure, the left number is the identification number of the centroid and the percentage indicates the number of hourly backward trajectories occurring in that cluster.

observation was in agreement with the reported eastward movement of the plume from Fukushima after the explosions (RIU, 2012; Takemura et al., 2011). Taking the circumference of the Earth at 37° N latitude (32.044 km) as reference to estimate the velocity of the plume, due to it crosses the study area, and circulation time of 21 days, the estimated average zonal velocity was estimated to be about 63 km/h.

To verify the transport of Fukushima originated radionuclides by surface westerlies, we calculated hourly forward trajectories from the Fukushima Daiichi nuclear power plant as well as hourly backward

trajectories at different sampling points throughout the world, taking the period in which radionuclides measurements were registered into account. This study was based on the computation of daily average paths (centroid) which represent the average path of a set of trajectories and, hence facilitate the understanding of the whole information that is inside in one set of hourly trajectories. Hourly forward and backward trajectories at a height of 1000 m and a temporal coverage of 8 days were computed in each reference site around the world. After the set of backward trajectories have been computed, the cluster technique implemented in the HYSPLIT model, based on grouping backward trajectories by considering the trajectory endpoints (latitude and longitude), was used to simplify and understand this large quantity of information.

The analysis of the air mass forward movements during 12th -16th March showed that the air mass was displaced eastward from the Fukushima area and bifurcated into a northern and a southern branch outside of Japan (Fig. 3). This eastward bifurcation of air masses is in agreement with the simulation of the potential dispersion of the radioactive cloud after the nuclear accident of Fukushima (Weather Online Website of United Kingdom, UK, 2012).

On 16th March the air mass over Fukushima moved from easterly to south-easterly direction by the presence of a high pressure system in the west and a low pressure system in the east of Fukushima on 16th March (Fig. 4a) and reached the Southeast Asia as shown in Stohl et al. (2012) and Long et al. (2012). However, the progressive weakening of the low pressure system in the east of Fukushima during the following days (Fig. 4b) was in favour to limit the influence of this branch over South Korea. This analysis indicated the progressive arrival of a strong high pressure system from the west, reaching a defined and stable location over eastern Asia during this period, being in favour to the non-existence of any wind corridor from Fukushima area to South Korea at surface level during this period. It is noted, although, that in annual average, the area encompassing Japan, Korean Peninsula, and eastern and southern part of China close to Vietnam is under the influence of the same air

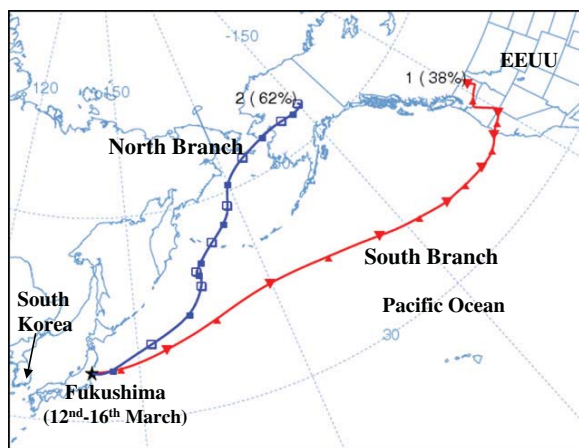


**Fig. 3.** The two main air mass branches (centroids) from Fukushima Daiichi nuclear power plant from 12th to 16th March. Each centroid has a temporal coverage of 192 hours (8 days) and initial height of 1000 m. The number is the identification number of the centroid and the percentage indicates the number of hourly backward trajectories occurring in that cluster. 1 and 2 in the figure stands for the south and north branches of the Fukushima radioactive plume.

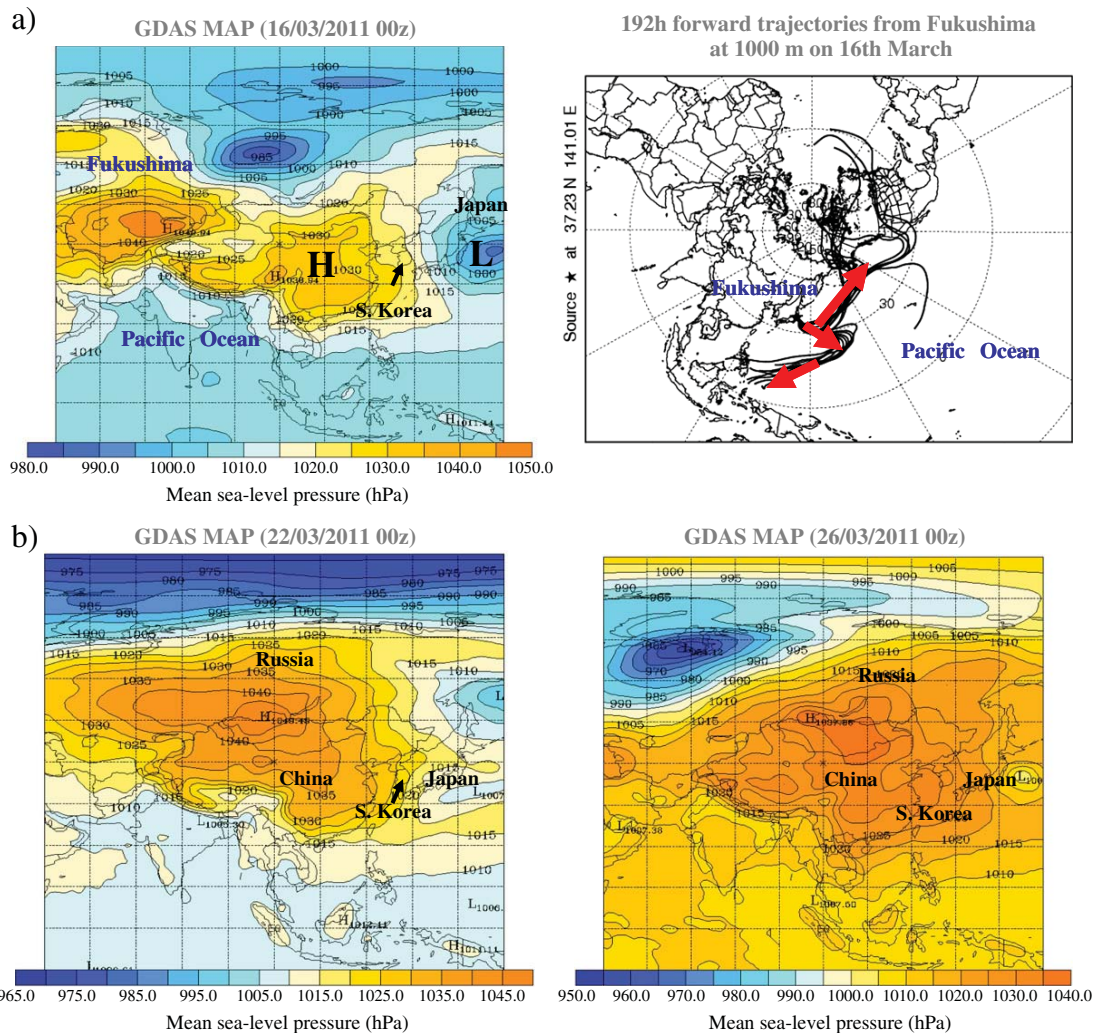


Fig. 4. a) Synoptic chart and 192 hours forward trajectory from Fukushima nuclear plant on 16th March 2011 and b) synoptic charts on 22nd and 26th March 2011. H means high-pressure area and L means low pressure area.

system as evidenced by the atmospheric concentration of  $^{133}\text{Xe}$  emitted from nuclear power plants in South Korea and Japan (Achim et al., 2011).

The southern branch air mass from Fukushima (Fig. 3), with a frequency of 38 %, was displaced in the marine boundary layer toward western North America, located more than 7000 km away, and arrived at the west coast of North America on March 16th (Bowyer et al., 2011; Sinclair et al., 2011; Diaz Leon et al., 2011). This southern branch arrived later in southern Europe, with peak concentrations at the south western Iberian Peninsula on 27th–28th March (Lozano et al., 2011; Masson et al., 2011).

The northern branch air mass, with a nearly double occurrence frequency (62%), was displaced to higher latitudes (Fig. 3). US E.P.A (2011) measurements over sampling sites in Alaska confirmed this movement of the plume. The analysis of backward trajectories indicated that this displacement was attributed to the arrival of  $^{131}\text{I}$  between 19th– 20th March in Iceland and from 21st March in the northern part of Scandinavia (Masson et al., 2011). The concentrations in Europe registered at Krakow (Poland) on 28th March were found to have originated from the same air mass that arrived earlier in Iceland, and 24th March in Greece (Manolopoulou et al., 2011), which indicated the limited influence of the southern branch air mass in southern Europe (Fig. 5). After the dispersion of the northern

Europe, Fukushima radioactive plume subsequently arrived over the center of Asia registering the highest activity concentration (by the analysis of melted snow sample) on 4th April (Bolsunovsky and Dementyev, 2011). This activity concentration in the centre of Asia was also in agreement with the backward trajectory results obtained for South Korea, thereby closing the global transport of the plumes northern branch. Taking into account the cumulative uncertainties caused by the computation of trajectories with a large temporal coverage (Stohl, 1998), Fig 5 shows the set of air masses that connect the Fukushima area and the surroundings of S. Korea during 12nd–16th March, confirming the origin of the activity concentrations in Korea and in Europe during March 11th (Masson et al., 2011).

#### 4. Conclusions

The unique global coverage of fallout radiocaesium released from the Fukushima Daiichi Nuclear Power Plant, particularly a fresh injection of  $^{134}\text{Cs}$  and  $^{137}\text{Cs}$  to the ground air provided a rare opportunity to observe a complete, uninterrupted revolution of the mid-latitude Surface Westerlies of the northern Hemisphere in late March 2011. This revolution took less than 21 days. This occurrence was verified for the first time based on the simultaneous global surface air measurements of artificial radionuclides, e.g.,  $^{131}\text{I}$ ,  $^{134}\text{Cs}$ , and  $^{137}\text{Cs}$ , and using the HYSPLIT model.

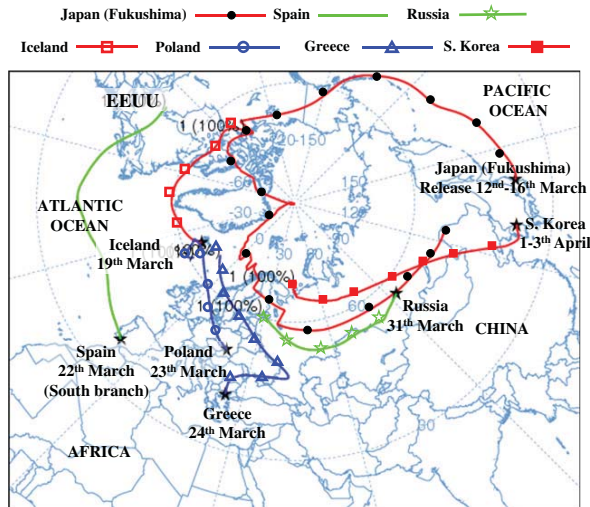


**Fig. 5.** The centroids of the 8 days backward trajectory analysis at different sites around the world indicating the transport of the Fukushima plume and the centroid of the 19 days forward trajectories from Fukushima from 12th to 16th of March. The number 1 is the identification number of the centroid and the percentage (100%) indicates the number of hourly backward trajectories occurring in that cluster.

This work clearly demonstrates how little dissipation occurred during this time due to the nature of the rapid global air circulation system, and the Fukushima radioactive plume contaminated the entire Northern Hemisphere during a relatively short period of time. The westerlies have strengthened and shifted pole ward over the past 50 years probably due to atmospheric warming arising from the increasing concentrations of atmospheric carbon dioxide (Anderson et al., 2009; Toggweiler, 2009), therefore a close look at the depositional fluxes of Fukushima released radionuclides over the earth surface would help in providing a better understanding of the dynamics of the northern Hemisphere westerlies.

### Acknowledgements

The authors are grateful to two anonymous reviewers for their constructive comments and criticism, and by taking their suggestions, our manuscript was significantly improved. This work is partly sponsored by the Korea Ocean R & D Institute (PE98564 & PE98743) to GHH, YIK, HML, SHK, and also partially supported by the Spanish Department of Science and Technology through the project “Determination of scavenging rates and sedimentation velocities using reactive-particle radionuclides in coastal waters; application to pollutants dispersion” (Ref.: CTM2009-14321-C02-01), and the Government of Andalusia project “Characterization and modelling of the phosphogypsum stacks from Huelva for their environmental management and control” (Ref.: RNM- 6300) to JPB, MAHC and RLL. The authors gratefully acknowledge the NOAA Air Resources Laboratory (ARL) for the provision of the HYSPLIT transport and dispersion model used in this publication.

### References

Achim P, Gross P, Le Petit G, Taffary T, Armand P. Contribution of isotopes production facilities and nuclear power plants to Xe-133 worldwide atmospheric background. S&T CTBTO; 2011.

Anderson RF, Ali S, Bradtmiller LI, Nielsen SHH, Fleisher MQ, Anderson BE, et al. Wind-Driven Upwelling in the Southern Ocean and the Deglacial Rise in Atmospheric CO<sub>2</sub>. *Science* 2009;323:1443.

Bolsunovsky A, Dementyev D. Evidence of the radioactive fallout in the center of Asia (Russia) following the Fukushima Nuclear Accident. *J Environ Radioact* 2011;102:1062–4.

Bowyer TW, Biegalski SR, Cooper M, Eslinger PW, Haas D, Hayes JC, et al. Elevated radionuclides on detected remotely following the Fukushima nuclear accident. *J Environ Radioact* 2011;102:681–7.

Diaz Leon J, Jaffe DA, Kaspar J, Knecht A, Miller ML, Robertson RG, et al. Arrival time and magnitude of airborne fission products from the Fukushima, Japan, reactor incident as measured in Seattle, WA, USA. *J Environ Radioact* 2011;102:1032–8.

Draxler RR, Stunder B, Rolph G, Taylor A. HYSPLIT\_4 User's Guide, via NOAA ARL Website. Silver Spring, MD: NOAA Air Resources Laboratory; 2009. Dec., 1997, revised Jan., [http://www.arl.noaa.gov/documents/reports/hysplit\\_user\\_guide.pdf](http://www.arl.noaa.gov/documents/reports/hysplit_user_guide.pdf).

Gridded Meteorological Data Archives. HYSPLIT Website, via NOAA ARL Website. <http://ready.arl.noaa.gov/archives.php> (last accessed: 23 January, 2012).

Hernández-Ceballos, M.A., Adame, J.A., Bolívar, J.P., De la Morena, B.A. Vertical behaviour and meteorological properties of air masses in the southwest of the Iberian Peninsula (1997–2007). *Meteorology and Atmospheric Physics in revision*.

Hong GH, Chung CS, Lee SH, Kim SH, Baskaran M, Lee HM, et al. Artificial radionuclides in the Yellow Sea: Inputs and redistribution. *Radioact Environ* 2006;8:96–133.

Hong GH, Hernández-Ceballos MA, Lozano RL, Kim YI, Lee HM, Kim SH, Yeh SW, Bolívar JP, Baskaran M. Radioactivity impact in South Korea from the damaged nuclear reactors in Fukushima: and evidence of the long and short transports. *J Radiol Prot* in press.

Kim CK, Byun JI, Chae JS, Choi HY, Choi SW, Kim DJ, et al. Radiological impact in Korea following the Fukushima nuclear accident. *J Environ Radioact* 2011. <http://dx.doi.org/10.1016/j.envrad.2011.10.018>.

KINS (Korea Institute of Nuclear Safety). Website [www.kins.re.kr/2011](http://www.kins.re.kr/2011) (last accessed : 1 February, 2012).

Lee YK, Kim SH, Hong GH, Lee KW. A study on the atmospheric deposition of radionuclides (<sup>137</sup>Cs and <sup>210</sup>Pb) on the Korean Peninsula. *J Korea Air Pollut Res Assoc* 1995;11:351–9 (in Korean).

Long NQ, Truong Y, Hien PD, Binh NT, Sieu LN, Giap TV, et al. Atmospheric radionuclides from the Fukushima Dai-ichi nuclear reactor accident observed in Vietnam. *J Environ Radioact* 2012. <http://dx.doi.org/10.1016/j.envrad.2011.11.018>.

Lozano RL, Hernández-Ceballos MA, Adame JA, Casas-Ruiz M, Sorribas M, San Miguel EG, et al. Atmospheric routes involved in the radioactive impact of Fukushima accident on the Iberian Peninsula. *Environ Int* 2011;37:1259–64.

Machta L, List RJ, Huber LF. World-wide travel of atomic debris. *Science* 1956;124:474.

Manolopoulou M, Vagena E, Stoulos S, Ioannidou A, Papastefanou C. Radioiodine and radiocesium in Thessaloniki, Northern Greece due to the Fukushima nuclear accident. *J Environ Radioact* 2011;102:796–7.

Masson O, et al. Tracking of airborne radionuclides from the damaged Fukushima Dai-ichi nuclear reactors by European networks. *Environ Sci Technol* 2011;45:7607–77.

Minoura K, Imamura F, Sugawara D, Kono Y, Iwashita T. The 869 Jogan tsunami deposit and recurrence interval of large-scale tsunamis on the Pacific coast of northeast Japan. *J Nat Disaster Sci* 2001;23:83–8.

Momoshima N, Sugihara S, Ichikawa R, Yokohama H. Atmospheric radionuclides transported to Fukuoka, Japan remote from the Fukushima Daiichi nuclear power complex following the nuclear accident. *J Environ Radioact* 2012:28–32.

Priyadarshi A, Dominguez G, Thiemens MH. Evidence of neutron leakage at the Fukushima nuclear plant from measurements of radioactive <sup>35</sup>S in California. *Proc Natl Acad Sci* 2011;109:14422–5.

RIU. Rhenish Institute for Environmental Research at the University of Cologne. Website <http://www.wurad.uni-koeln.de/indexe.html> (last accessed : 15 January, 2012).

Seinfeld JH, Pandis SN. *Atmospheric Chemistry and Physics: From air pollution to climate change*. New York: John Wiley and Sons; 2006. 1232 pp.

Sinclair LE, Seywerd HCJ, Fortin R, Carson JM, Sault PRB, Coyle MJ, et al. Aerial measurement of radionuclide concentration off the west coast of Vancouver Island following the Fukushima reactor accident. *J Environ Radioact* 2011;102:1018–23.

Steffensen JP, Andersen KK, Bigler M, Clausen HB, Dahl-Jensen D, Fisher H, et al. High-resolution Greenland ice core data show abrupt climate change happens in few years. *Science* 2008;321:680–4.

Stohl A. Computation, accuracy and applications of trajectories-A review and bibliography. *Atmos Environ* 1998;32:947–66.

Stohl A, Seibert P, Wotawa G, Arnold D, Burkhardt JF, Eckhardt S, et al. Xenon-133 and caesium-137 releases into the atmosphere from the Fukushima Dai-ichi nuclear power plant: determination of the source term, atmospheric dispersion, and deposition. *Atmos Chem Phys* 2012;12:2313–43.

Stunder B. An assessment of the Quality of Forecast Trajectories. *J Appl Meteorol* 1996;35:1319–31.

Takemura T, Nakamura H, Takigawa M, Kondo H, Satomura T, Miyasaka T, et al. A numerical simulation of global transport of atmospheric particles emitted from the Fukushima Daiichi nuclear power plant. *SOLA* 2011;7:101–4.

Toggweiler JR. Shifting Westerlies. *Science* 2009;323:1434.

Uno I, Eguchi K, Yumimoto K, Takemura T, Shimizu A, Uematsu M, et al. Asian dust transported one full circuit around the globe. *Nat Geosci* 2009;2:557–60.

US E.P.A. (United States Environmental Protection Agency). Website <http://www.epa.gov/japan2011/rert/radnet-sampling-data.html> (last accessed : 10 January, 2012).

Weather Online Website of United Kingdom (UK). Website <http://www.weatheronline.co.uk/> (last accessed: 27 February, 2012).